ELSEVIER

Chemical Engineering Journal 133 (2007) 151–156

Chemical Engineering Journal

www.elsevier.com/locate/cej

Determination of the kinetic and equilibrium parameters of the *n*-boc-rolipram enantiomers on a chiral stationary phase by high performance liquid chromatography

C.V. Gonçalves [a,*], M.J.S. Carpes [b], C.R.D. Correa [b], C.C. Santana [a]

[a] *Universidade Estadual de Campinas, Faculdade de Engenharia Química, Departamento de Processos Biotecnológicos, Albert Einstein 500 – Campinas, SP, CEP 13081-970, Brazil*

[b] *Universidade Estadual de Campinas, Instituto de Química, Departamento de Química Orgânica, Josué de Castro S/N – Campinas, SP, CEP 13081-970, Brazil*

Received 11 May 2006; received in revised form 22 February 2007; accepted 1 March 2007

Abstract

The kinetic and equilibrium parameters for the chromatographic separation of racemate *n*-boc-Rolipram, using cellulose tris(3,5-dimethylphenylcarbamate) supported on silica as the chiral stationary phase and hexane/2-propanol as the mobile phase, were evaluated by moment analysis basing on equilibrium-dispersive and linear driving force models. The overall mass transfer coefficients and equilibrium constants were evaluated for both enantiomers. Others parameters, required to evaluate the bed performance, such as bed voidage and the axial dispersion coefficient, were also determined. The results show that diffusion dynamic plays an important role on the separation process of the both enantiomers. These parameters are very important for the design of continuous preparative chromatography like simulated moving bed (SMB).

Keywords: *n*-boc-Rolipram; Cellulose tris(3,5-dimethylphenylcarbamate) supported on silica; HPLC; Equilibrium parameters; Kinetic parameters

1. Introduction

Rolipram is a compound with a varied biological activity. In particular, attention has been drawn to the emetic [1], anti-inflamatory [2], immunosupressant [3], antidepressive [4,5], putative antiparkinsonian [6], and neuroprotective [7] effects. The best characterized biochemical activity of the Rolipram is the selective inhibition of the cAMP-selective phosphodiesterase family known as Type IV (PDE4). Its selectivity for this subtype of phosphodiesterases is the hallmark of classification of these enzymes [8]. Phosphodiesterases (PDEs) are a family of enzymes responsible for the hydrolysis of intracellular messengers, cyclic AMP (cAMP) and cyclic GMP (cGMP), causing their inactivation. The cyclic nucleotides adenosine 3′5′ monophosphate (cAMP) and guanosine 3′5′ monophosphate (cGMP) are critical intracellular signaling molecules controlling the inflammatory cell function. PDE 4 is a specific cAMP and is localized in airway smooth muscles, all inflammatory cells and the vascular endothelium [9].

The biological activity of Rolipram enantiomers is wide divergent and the (*R*)-Rolipram tends to be more potent than the (*S*)-Rolipram [10–14]. The structure of the two enantiomers is shown in Fig. 1.

Racemic drugs separations using chiral stationary phase (CSP) by continuous chromatographic method such as the simulated moving bed (SMB) have grown considerable interest in the recent years. In this kind of enantioselective preparative chromatography, special attention is given, in particular, to loading capacity, which is a characteristic of the stationary phase, to flow-rate, which is limited by the mechanical resistance of the material at pressuring and its granulometry, and to feed concentration, which is often related to the solubility of the solute in the applied mobile phase [15]. The advantages of this method are its high selectivity, the simple product recovery, the ease of further purification and the very short product recovery time. For the optimization of each separation, some kinetic and equilibrium parameters are required.

* Corresponding author. Present address: Universidade Federal do Ceará, Departamento de Engenharia Química, Campus do Pici S/N – Fortaleza, CE, CEP 60455-760, Brazil. Tel.: +55 85 3366 9611 26; fax: +55 85 3366 9611 26.
E-mail address: caroline@gpsa.ufc.br (C.V. Gonçalves).

1385-8947/$ – see front matter © 2007 Elsevier B.V. All rights reserved.
doi:10.1016/j.cej.2007.03.001

Nomenclature

$(Bi)_m$	Biot number
c	concentration of adsorbate in fluid phase
c_0	initial concentration of adsorbate in fluid phase
c^F	feed concentration of adsorbate
d_p	particle diameter
D_c	micropore diffusivity
D_L	axial dispersion coefficient
D_m	molecular diffusivity
D_p	pore diffusivity
H	dimensionless equilibrium constant
HETP	height equivalent theoretical plate
k_f	mass transfer coefficient outside of the particle
K_L	overall mass transfer coefficient
L	bed length
N	theoretical plate number
q	adsorbate concentration in adsorbed phase
$\bar{q}$	media adsorbate concentration in adsorbed phase
r_c	crystal radius
R_p	particle radius
Sh	Sherwood number
t	time
t_{oR}	mean retention time for an unretained compound
u	superficial velocity
x, z	coordinates

Greek letters

$\delta(t)$	Dirac function
ε	bed voydage
ε_P	particle voydage
ε_T	global porosity
λ	flow geometry-dependent constant
μ	first moment of chromatographic response
ν	interstitial velocity
σ^2	second moment of the chromatographic response
τ	tortuosity

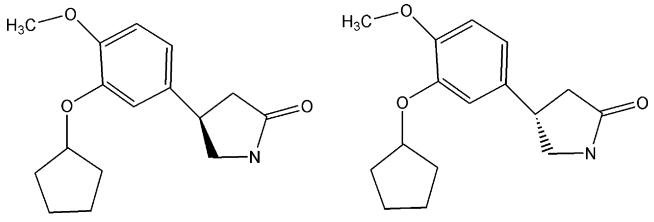

Fig. 1. Enantiomers of Rolipram [14].

The main objective of this study is a determination of kinetic and equilibrium parameters of the *n*-boc-Rolipram (Rolipram intermediary form) by the chromatographic method (moment analysis) on cellulose tris(3,5-dimethylphenylcarbamate) supported on silica (Fig. 2), which is used in continuous chromatographic systems such as SMB.

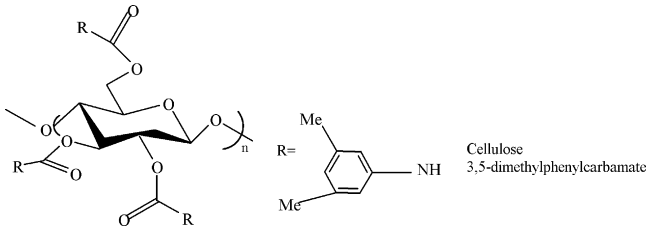

Fig. 2. Cellulose tris(3,5-dimethylphenylcarbamate).

2. Theoretical

2.1. The rate model of chromatography

To analyze and interpret data from a chromatographic experiment, a mathematical model is needed. Then, parameters characterizing the kinetics and the equilibrium of the sorption process can be experimentally derived by matching the observed response to the model predictions. The axial dispersed plug flow model can generally represent the flow of a fluid through a packed column. The basic continuity equation, derived from a mass balance on an element of the column, is [16]

$$-D_L\frac{\partial^2 c}{\partial z^2}+\frac{\partial}{\partial z}(vc)+\frac{\partial c}{\partial t}+\left(\frac{1-\varepsilon}{\varepsilon}\right)\frac{\partial \bar{q}}{\partial t}=0 \tag{1}$$

If the system is isothermal with negligible pressure drop and if the concentration of the adsorbable species is small, the fluid velocity may be considered as constant through the column and, under these conditions (Eq. (1)) simplifies to

$$-D_L\frac{\partial^2 c}{\partial z^2}+v\frac{\partial c}{\partial z}+\frac{\partial c}{\partial t}+\left(\frac{1-\varepsilon}{\varepsilon}\right)\frac{\partial \bar{q}}{\partial t}=0 \tag{2}$$

This is the form generally used in models of dynamic response of a chromatographic column.

The term $\partial\bar{q}/\partial t$ represents the local mass transfer rate averaged over an adsorbent particle. To obtain the dynamic response of the system [$c = c(z, t)$], it is necessary to solve (Eq. (2)) simultaneously with the appropriate mass transfer rate expression:

$$\frac{\partial \bar{q}}{\partial t}=f(c,q) \tag{3}$$

Subject to the initial and boundary conditions imposed on the system. For the pulse perturbation, this is:

$$c(z,0)=q(z,0)=0,\quad c(0,t)=c_0\delta(t) \tag{4}$$

In addition the "long column" condition,

$$c|_{z\to\infty}=0 \tag{5}$$

is usually assumed.

In the application of the chromatographic method to the measurement of intraparticle diffusivities, we are primarily concerned with linear systems so that equilibrium relationship may be expressed in the form

$$q^*=Hc \tag{6}$$

In practice, linearity can generally be achieved by keeping the magnitude of the concentration perturbation small.

2.2. Moment analysis

The hydrodynamics of a chromatographic column can be described through the analysis of the residence-time distribution of the eluent, which is classically derived from the response curve to a Dirac injection. This response curve of the column to a Dirac injection contains information associated with the properties of the column [17]. These properties, which include the equilibrium and mass transfer parameters, can be extracted by several methods: solution in the time domain, solution in the Laplace domain, solution of the Fourier domain and the method of moments [18]. Ramachandran and Smith [19] discussed the merits and limitations of each method. Parameter estimations by the method of moments have been covered in details previously [20–22].

The expressions for the moments of the chromatographic response in terms of the model parameters may be derived directly from the solution of the model equations in Laplace form, by application of van der Laan's theorem [23]. The moments of the experimental response may be calculated directly by integration:

$$\text{First moment}: \ \mu \equiv \bar{t} = \int_0^\infty \frac{ct\,\mathrm{d}t}{\int_0^\infty c\,\mathrm{d}t} = -\lim_{s\to\infty}\frac{\partial\tilde{c}}{\partial s}\frac{1}{c_0} \tag{7}$$

$$\text{Second moment}: \sigma^2 \equiv \int_0^\infty \frac{c(t-\mu)^2\mathrm{d}t}{\int_0^\infty c\,\mathrm{d}t} = \lim_{s\to\infty}\frac{\partial^2\tilde{c}}{\partial s^2}\frac{1}{c_o} - \mu^2 \tag{8}$$

The expressions for the first and second moments of the pulse response for a simple LDF model in the linear region are expressed by Eqs. (9) and (10), respectively:

$$\mu = \frac{L}{v}\left[1 + \left(\frac{1-\varepsilon}{\varepsilon}\right)H\right] \tag{9}$$

$$\sigma^2 = \frac{2D_L}{u}\left\{\frac{D_L}{u^2}\left[1 + \left(\frac{1-\varepsilon}{\varepsilon}\right)H\right]^2 + \left(\frac{1-\varepsilon}{\varepsilon}\right)\frac{H}{K_L}\right\} \tag{10}$$

From the moment analysis of the solution on the general rate model in the Laplace domain, we can obtain the expression for the height equivalent to a theoretical plate (HETP) [20], which equals

$$\mathrm{HETP} = \frac{L}{N} = \frac{\sigma^2}{\mu^2}L \tag{11}$$

From Eqs. (9) and (10) combined with Eq. (11), we obtain:

$$\mathrm{HETP} = \frac{2D_L}{u} + 2u\left(\frac{1-\varepsilon}{\varepsilon}\right)\frac{H}{K_L}\left[1 + \left(\frac{1-\varepsilon}{\varepsilon}\right)H\right]^{-2} \tag{12}$$

The overall mass transfer resistance ($1/K_L$) includes external film, micro and macropores diffusional resistances [16]:

$$\frac{1}{K_L} = \frac{R_P}{3k_f} + \frac{R_P^2}{15\varepsilon_P D_P} + \frac{r_c^2}{15\mathrm{HD}_c} \tag{13}$$

The magnitude of the term that describe external film's formation on particle at the mass transfer resistance could be evaluated by the $(Bi)_m$ written according to Sherwood number:

$$(Bi)_m = \frac{Sh}{6}\frac{D_m}{\varepsilon_P D_P} \tag{14}$$

For $Sh \geq 2$ and $D_P \leq D_m/\tau$, the $(Bi)_m$ assume its minimum value:

$$(Bi)_m = \frac{\tau}{3\varepsilon_P} \tag{15}$$

Under these conditions, the intern concentration gradient is larger than the extern gradient. Any additional resistance to the mass transfer will reduce the D_P appreciably. Thus, the mass transfer resistance inside the particle is more important than that one associated with the external film's formation on the particle at the mass transfer rate [20].

The silica used in this work as support of the cellulose tris(3,5-dimethylphenylcarbamate) is a mesoporous material, thus the term referred to the diffusion in micropores was neglected as well. Therefore, only the second term of Eq. (13) has a considerable meaning in the calculus of the K_L:

$$\frac{1}{K_L} = \frac{R_P^2}{15\varepsilon_P D_P} \tag{16}$$

2.3. Axial dispersion in packed beds

The source of band broadening of a kinetic origin includes molecular diffusion, eddy diffusion, the mass transfer resistances and the finite rate of kinetics of adsorption–desorption [24]. When we are modelling chromatography, the phenomena that contribute to axial mixing are included in a single axial dispersion coefficient. The two main mechanisms contributing to axial dispersion are molecular diffusion and eddy diffusion. In a first order approximation, the two contributions are additive and D_L is given by Eq (17):

$$D_L = \gamma_1 D_m + \gamma_2 d_P u \tag{17}$$

where D_m is the molecular diffusivity, d_P, the average particle size and u is the mobile phase velocity. γ_1 and γ_2 are geometrical constants, usually around 0.7 and 0.5, respectively [24].

Dispersion under linear conditions is characterized by the height equivalent to theoretical plate (HETP) in the equilibrium-dispersive model. The HETP concept is strictly valid only when the rate of the mass transfer kinetics is relatively fast and the profile of the elution peak is a Gaussian. Therefore, D_L can be calculated by Eq. (12) [16].

3. Experimental

3.1. Materials and equipment

n-boc-Rolipram enantiomers, in their free-base form, were kindly supplied by the Chemical Institute of UNICAMP. Tri-*tert*-butylbenzene (TTBB) was purchased from Aldrich, and hexane and propanol-2, both HPLC grade, from Malinckrodt and J.T. Baker, respectively.

The experiments were carried out using a single liquid chromatographic system. The chromatographic column (0.45 cm × 25 cm) was packed using cellulose tris(3,5-dimethylphenylcarbamate) supported on silica as chiral stationary phase. The experimental set-up consisted of two WATERS HPLC pumps, a WATERS UV-detector set at 270 nm, equipped with a Rheodyne model 9125 sample injector and a data acquisition system.

3.2. Chromatographic experiments

TTBB and the two enantiomers of the *n*-boc-Rolipram were dissolved separately in the mobile phase (hexane/2-propanol 90:10, v/v), which were degassed in an ultrasonic bath.

A typical chromatographic experiment consists in an injection, in a chromatographic column previously saturated and stabilized with the mobile phase, a small pulse of adsorbate (20 μL) in a given flow rate and temperature. Several response peaks were measured at different flow rates of the mobile phase. For each response peak, the first and the second moment were calculated. These response peaks gave complete data about the determination of the adsorption equilibrium and kinetic parameters.

The first moment is plotted versus L/u and HETP versus u. Both plots should produce a straight line. Henry constant is found in agreement with Eq. (9) and HETP is found in agreement with Eq. (11).

3.3. Determination of the global, particle and bed voydage

The usual definition of the mean residence time in chromatography is given by Eq. (18)

$$t_{oR} = \frac{\varepsilon_T L}{u} \tag{18}$$

where u and L are the superficial velocity and column length, respectively, and ε_T is the global porosity of the bed. In order to determinate the global porosity of the bed, 1 mg/ml of the 1,3,5 TTBB tracer was injected in the column and the ε_T was calculated by Eq. (18).

Bed voydage was calculated by the correlation given by RUTHVEN [20] and SUZUKI [21]:

$$\varepsilon_T = 0.45 + 0.55\varepsilon \tag{19}$$

where ε is the bed voydage and ε_T is global voydage.

The voydage of the particle was calculated by Eq. (20):

$$\varepsilon_P = \frac{\varepsilon_T - \varepsilon}{1 - \varepsilon} \tag{20}$$

3.4. Determination of axial dispersion coefficient

In this work, all the effects which contribute to the axial mixing were include in a single effective axial dispersion coefficient calculated by Eq. (17). In liquid phase, the molecular diffusivity is too small to contribute significantly on the axial dispersion coefficient, even at low Reynolds numbers [20]. Therefore, in this work, the molecular diffusivity can be neglected. Eq. (17) can be written in this way:

$$D_L = \gamma_2 d_P u = \lambda u \tag{21}$$

Combining Eqs. (12) and (17), we obtain:

$$\mathrm{HETP} = 2\lambda + 2u\left(\frac{1-\varepsilon}{\varepsilon}\right)\frac{H}{K_L}\left[1 + \left(\frac{1-\varepsilon}{\varepsilon}\right)H\right]^{-2} \tag{22}$$

where λ is defined according to Eq. (23):

$$\lambda = \frac{2D_L}{\nu} \tag{23}$$

4. Results and discussion

4.1. Determination of the bed voydage and axial dispersion coefficient

Global voidage ε_T, was found to be 0.56, by Eq. (18); the bed voydage ε (calculated by Eq. (19)) of chiral column was 0.20. Particle voidage, necessary to determinate the diffusivity (calculated by Eq. (20)) was found to be 0.45. The experimental and calculated values show a chiral bed well packed resulting in a large number of theoretical plates.

The axial dispersion coefficient was calculated by Eq. (23) from linear coefficient obtained by the plot of HETP versus the superficial velocity shown in Fig. 3 (Fig. 3). The value was found to be 0.02ν on the chiral bed, i.e., small axial dispersion coefficient. Both results, porosities and axial dispersion, demonstrate good performance of the method used to pack the bed.

4.2. Determination of the kinetic and equilibrium parameters

Figs. 4 and 5 show plots of first moment versus L/u and HETP versus u for *R*-boc-Rolipram at 25 °C (Figs. 4 and 5).

Figs. 6 and 7 show plots of first moment × L/u and of HETP versus u for *S*-boc-Rolipram at 25 °C (Figs. 6 and 7).

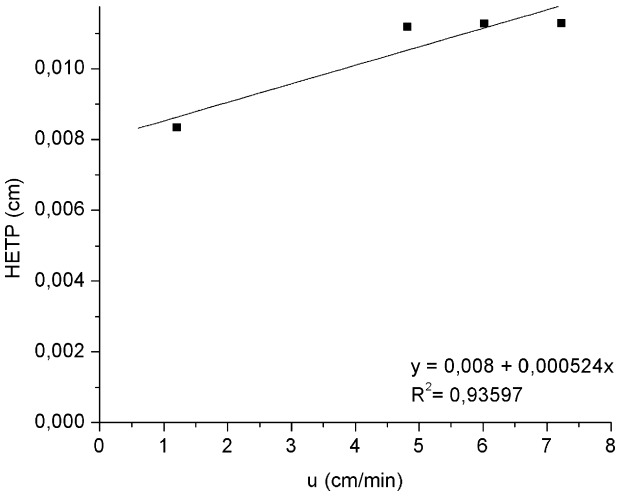

Fig. 3. HETP vs. u of the TTBB on the chiral column.

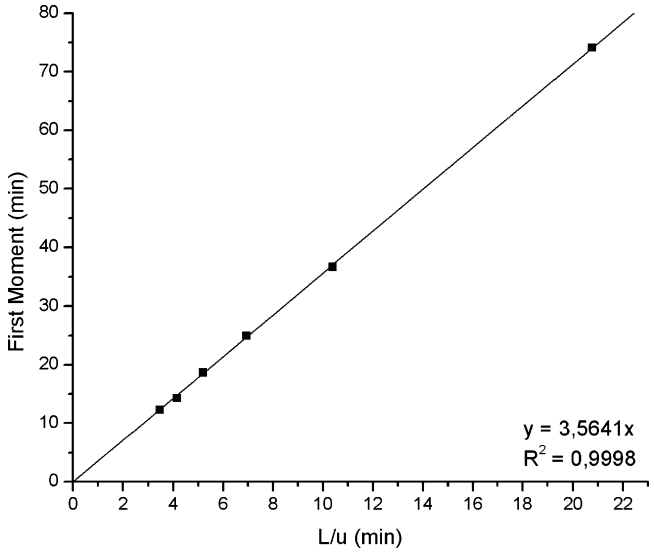

Fig. 4. First moment vs. *L*/*u* of *R*-boc-Rolipram.

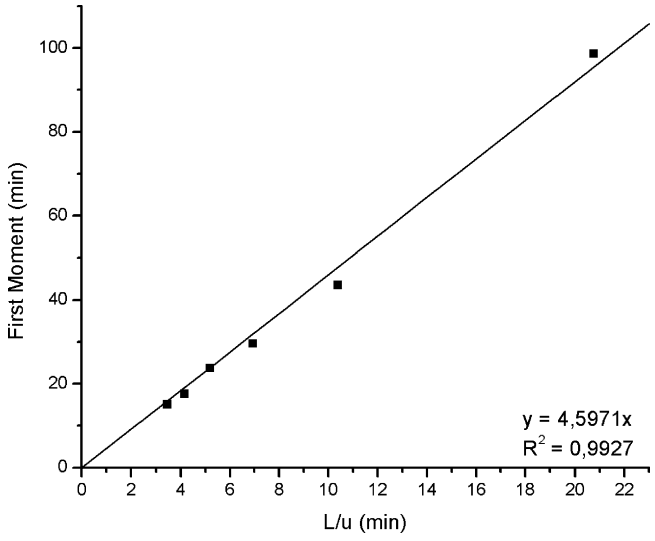

Fig. 6. First moment vs. *L*/*u* of *S*-boc-Rolipram.

Henry constants of the *R* and *S*-boc-Rolipram were calculated by Eq. (9) from the angular coefficient of the plot shown in Figs. 4 and 6.

The HETP to each enantiomer (*R* and *S*) was found by Eq. (11). From the angular coefficient obtained by the plot of HETP versus *u* (Figs. 5 and 7), it was possible to calculate, according to Eq. (12), the mass transfer coefficient.

The plots of HETP versus the superficial velocity for the two enantiomers in Figs. 5 and 7 show that HETP increases approximately linearly with the velocity (the pairs of datas that appear almost in line and parallel to the *x*-axis can be attributed mainly to experimental errors).

The diffusivity of the two enantiomers was calculated according to Eq. (16). Measurements carried out by light-scattering of the chiral stationary phase provided an average particle size of 11.67 μm. The equilibrium and kinetic parameters measured are shown in Table 1.

Although the equilibrium constant of *R*-boc-Rolipram was smaller than *S*-boc-Rolipram, which means a small interaction with the synthesized CSP, its diffusivity, calculated from K_L,

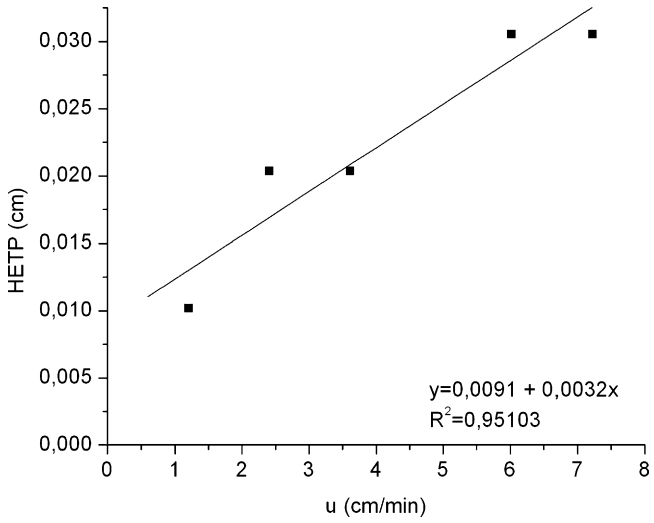

Fig. 5. HETP vs. u of *R*-boc-Rolipram.

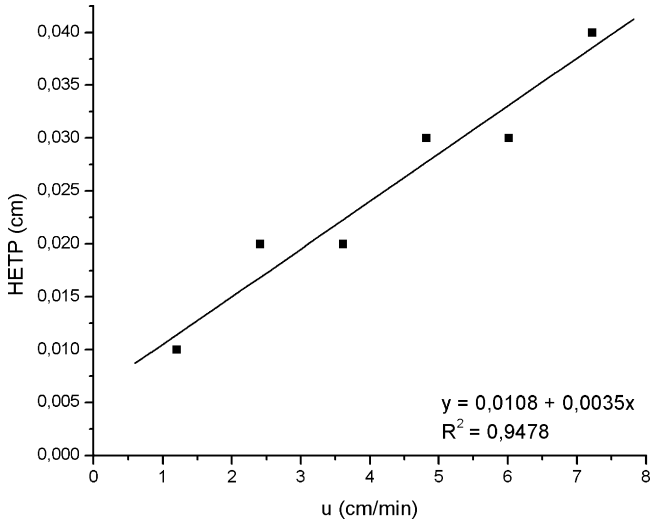

Fig. 7. HETP vs. *u* of *S*-boc-Rolipram.

Table 1
Kinetic and equilibrium parameters of the enantiomers

	Number of theoretical plates, *N*	Axial dispersion, D_L	Equilibrium constant, *H*	Mass transfer coefficient, K_L (s^{-1})	Pore diffusivity, D_P ($cm\ s^{-2}$)
R-boc-Rolipram	1134	0.02*v*	4.21	1.14	5.68×10^{-7}
S-boc-Rolipram	903	0.02*v*	5.50	0.79	5.16×10^{-8}

was larger than *S*-boc-Rolipram. This fact influences the number of necessary theoretical plates to separate the enantiomers of the racemic mixture; i.e., *R*-boc-Rolipram diffuses more quickly through the pores of the stationary phase, resulting in numerous interactions with synthesized CSP.

A suggested hypothesis to explain this phenomenon was that the spatial arrangement of *R*-boc-Rolipram would be positive to its diffusion inside the pores of the adsorbent and, at the same time, its adsorption on the synthesized CSP would be poor. The same hypothesis would be also valid for the *S*-boc-Rolipram, i.e., its spatial arrangement would not contribute positively to the diffusion inside the pores of the adsorbents, but it would favour its adsorption on the synthesized CSP.

Based on this hypothesis, we hope that *R*-boc-Rolipram will be better separated on this CSP than *S*-boc-Rolipram.

5. Conclusions

In this study, the overall mass transfer coefficient, diffusivities, axial dispersion coefficient, equilibrium constants of the two enantiomers and bed voidage of the column packed with cellulose tris(3,5-dimethylphenylcarbamate) supported on silica chiral stationary phase (CSP) for the separation of racemic *n*-boc-Rolipram were determined by moment analysis. The CSP shows a greater affinity for the *R* enantiomer of *n*-boc-Rolipram than for *S* enantiomer. The equilibrium and kinetic parameters of the *n*-boc-Rolipram enantiomers support an adsorption dynamics which favors the *R*-boc-Rolipram separation. Although, both the enantiomers shows a good affinity for the synthesized CSP, the diffusive process of enantiomers through the pores of cellulose tris(3,5-dimethylphenylcarbamate) supported in silica is crucial for the dynamics of the mass transfer.

Acknowledgements

The authors are grateful to CAPES (Coordenação de Aperfeiçoamento de Pessoal de Nível Superior), CNPq (Conselho Nacional de Desenvolvimento Científico e Tecnológico) and FAPESP (Fundação de Amparo a Pesquisa do Estado de São Paulo) for the financial support provided.

References

[1] R.J. Heaslip, D.Y. Evans, Eur. J. Pharmacol. 286 (1995) 281–290.
[2] L. Sekut, D. Yarnall, S.A. Stimpson, L.S. Noel, R. Bateman-Fite, R.L. Clark, M.F. Brackeen, J.A. Menius, K.M. Conolly, Clin. Exp. Immunol. 100 (1995) 126–132.
[3] N. Sommer, P.A. Loeschmann, G.H. Horthoff, M. Weller, A. Steinbrecher, J.P. Steinbach, R. Richtenfels, R. Meyermann, A. Reithmueller, A. Fontana, J. Dichgans, R. Martin, Nat. Med. 1 (1995) 244–248.
[4] M. Nibuya, E.J. Nestler, R.S. Duman, J. Neurosci. 16 (1996) 2365–2372.
[5] H.H. Schneider, R. Schimiechen, M. Brezinski, J. Seidler, Eur. J. Pharmacol. 127 (1986) 105–115.
[6] M. Casacchia, G. Meco, F. Castellana, L. Bedini, G. Cusimano, A. agnoli, Pharmacol. Res. Commun. 15 (1983) 329–334.
[7] H. Kato, T. Araki, Y. Itoyama, K. Kogure, Eur. J. Pharmacol. 272 (1995) 107–110.
[8] J.A. Beavo, D.H. Reifsnyder, Trends Pharmacol. Sci. 11 (1990) 150–155.
[9] A.M. Doherty, Curr. Opin. In Chem. Biol. 3 (1999) 466–473.
[10] J.E. Souness, L.C. Scott, Biochem. J. 291 (1993) 389–395.
[11] J. Semmler, H. Wachtel, S. Endress, Int. J. Immunopharmacol. 15 (1993) 409–413.
[12] J.E. Schultz, G. Folkers, Pharmacophysichiatry 21 (1998) 83–86.
[13] H.H. Schneider, M. Yamaguchi, J.S. Andrews, D.N. Stephens, Pharmacol. Biochem. Behav. 50 (1995) 211–217.
[14] J. Demnitz, L. La Vecchia, E. Bacher, T.H. Keller, T. Müller, F. Schürch, H.P. Weber, E. Pombo-Villar, Molecules 3 (1998) 107–119.
[15] E.R. Francotte, J. Chromatogr. A 906 (2001) 379–397.
[16] J. Kärger, D.M. Ruthven, Diffusion in Zeolites and Other Microporous Solids, John Wiley & Sons, New York, 1992, 605 p.
[17] G. Duan, C.B. Ching, S. Swarup, Chem. Eng. J. 69 (1998) 111–117.
[18] E.J. Kucera, Chroamtographia 19 (1965) 237.
[19] P.A. Ramachandran, J.M. Smith, Ind. Eng. Chem. Fundam. 17 (1978) 148.
[20] D.M. Ruthven, Principles of Adsorption and Adsorption Processes, Wiley, New York, 1984, 433 p.
[21] M. Suzuki, Adsorption Engineering, Elsevier, Amsterdam, 1990, p. 179.
[22] S. Yamamoto, K. Nakanishi, R. Matsuno, Ion-Exchange Chromatography of Proteins, Marcel Dekker, New York, 1988.
[23] E.R. Van der Laan, Chem. Eng. Sci. 7 (1958) 187.
[24] G. Guiochon, S. Golshan-Shirazi, A.M. Katti, Fundamentals of Preparative and Nonlinear Chromatography, Academic Press, Boston, 1994.